Biomimatic material(생체 모방 재료)의 공학적 응용 기술에 대한 연구동향

Chung-Ang University, Da Vinci College of General Education
OK JA Yoon

CHERIC
Chemical Engineering and Materials Research Information Center
국가지정
화학공학소재연구정보센터

연구 동향

✓ Biomimetic thermal-sensitive Multi-transform Actuator[1]

- 온도 감응형 액츄에이터 (thermo responsive hydrogel actuators)는 electrical Joule heating, photo-therma, exothermic reactions 등의 자극에 의해 부피나 형태가 변하기 때문에 다양한 분야에 응용되고 있음.

- 온도 감응형 하이드로 겔인 Poly N-isopropylacrylamide (PNIPAM)과 기능화된 *f*-PNIPAM은 서로 다른 온도의 낮은 임계 용액 온도 (LCST)를 나타내며 겔 부피 변화를 온도로 제어함.

- 자외선 가교 결합 (ultra-violet crosslinking) 기술을 이용하여 LCST에서 가열에 의해 특정 곡률로 굽히는 특성으로 가교 밀도 구배 제어가 가능한 겔 시트를 개발.

- 간단한 성형 공정을 사용하여 온도 변화에 따라 변하는 bio-inspired artificial flower과 같은 복잡한 모양 변화가 가능한 다중 변형 장치를 구성함.

- 차별화된 변형 자극과 간단한 몰딩 방법으로 여러 액추에이터를 사용하여 다중 변형 인공 근육 작동 구조 (multi-transform artificial muscle actuated structures)가 가능함을 보고하고 있으며 이러한 연구는 부드럽고 매끄러운 생체 모방 운동 및 소프트 로봇 연구에 적용될 것으로 기대됨.

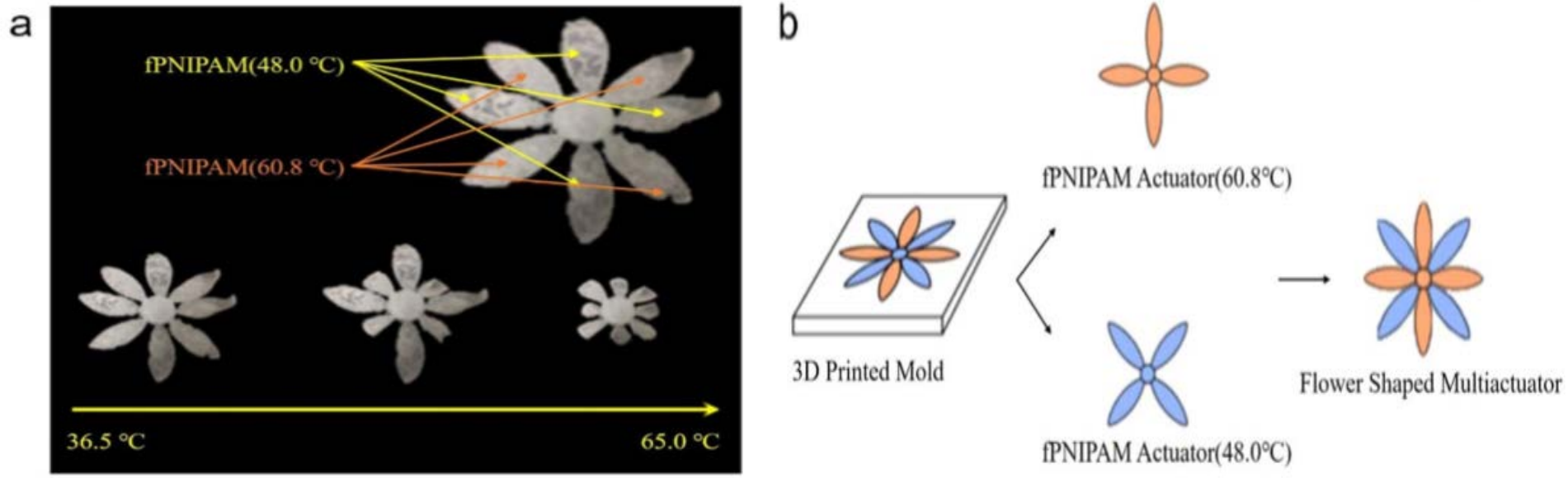

Figure 1. Flower blossom-shaped multi-transformation actuators. (**a**) Real-time image showing the different temperature-responsive actuation. The thickness of each actuator $t = 2$mm. The actuation occurs sequentially when the temperature rises. (**b**) Schematic image of the making process for the whole flower-type actuator structure. The two f-PNIPAM actuators, which have different LCSTs, were attached by *N*,*N*-bisacrylamide cross-linker.

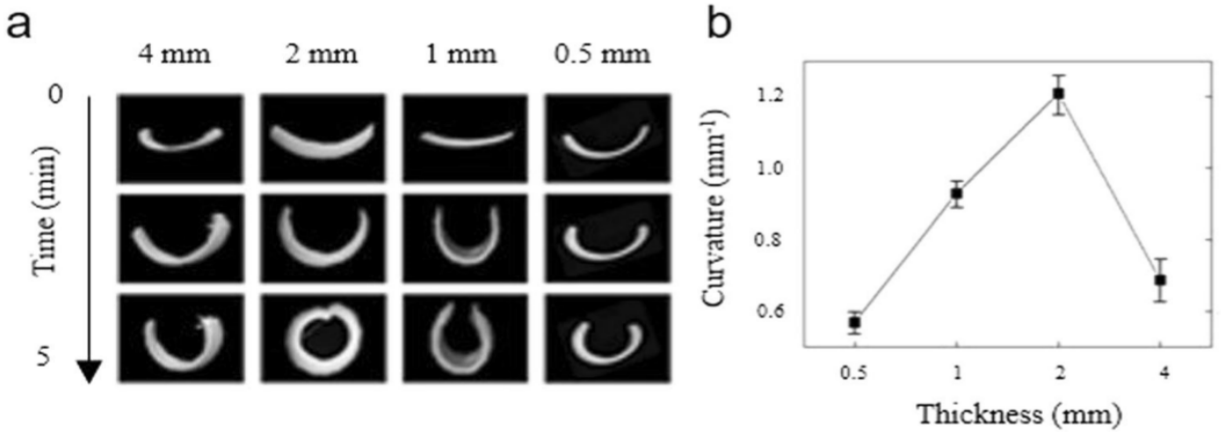

Figure 2. Actuation properties of f-PNIPAM prepared with different length: thickness ratios. The samples through the LCST caused bending away from the top surface. (**a**) Photographs during heating to above the LCST of four f-PNIPAM sheets prepared to the indicated length: thickness ratios. (**b**) Variation in the final curvature of the f-PNIPAM above the LCST as a function of the initial length: thickness ratio. The error bars represent the variation in the degree of curvature along the sample length.

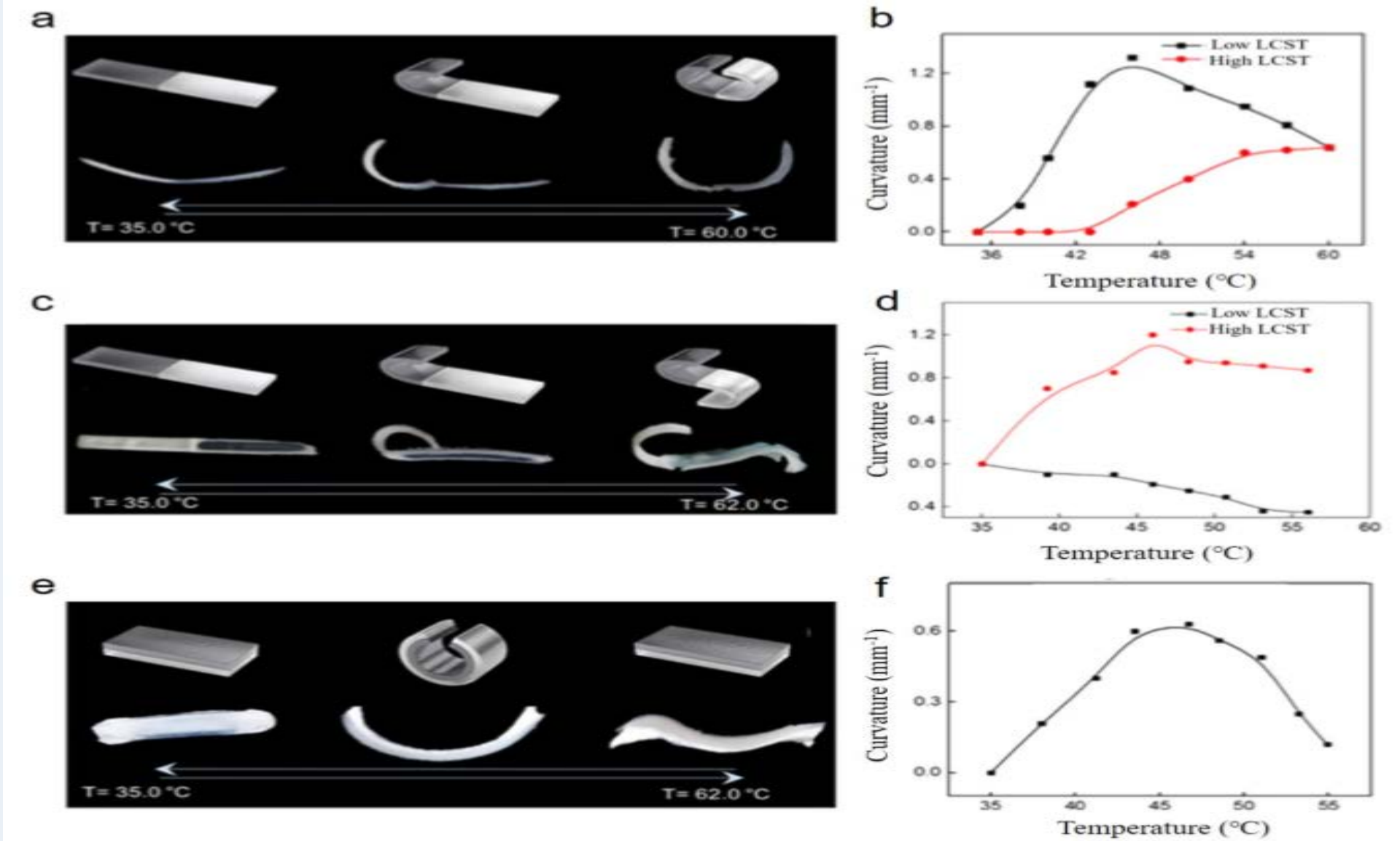

Figure 4. Diverse actuation by different LCST phase transitions. (**a**) The half-to-half structure consists of two different f-PNIPAMs which have low LCST (48.0 °C) and high LCST (60.8 °C). (**b**) Analysis of curvature change in (**a**) with increasing temperature. (**c**) Inverted half-to-half structure consisting of two different f-PNIPAMs with the opposite orientation in each half. One side has low LCST (48.0 °C) and the other side has high LCST (60.8 °C) (**d**) Analysis of curvature change in (**c**) with increasing temperature. (**e**) Structure of layer-on-layer and (**f**) its curvature analysis.

✓ A Study on the Mold Cooling Circuit Configuration Method Applying Biomimetics[2]

- 직선형 냉각관의 단점을 보완하고자 제품 표면을 따라가면서 냉각관이 배치되는 형상 적응형 냉각회로가 개발되고 있으며 유동 정체와 같은 문제로 냉각효율이 낮아지는 문제점이 발생하고 있음.
- 이러한 문제를 해결하기 위해 자연 상에 존재하는 식물의 뿌리나 사람의 혈관 형상에서는 유동 정체현상이 없으며 생성 원리 또한 단순하므로 이러한 원리를 모방하여 개발하고 있음.
- 식물의 뿌리가 일정 영역에서 양분이 소진될 경우 새로운 영역으로 성장해 나가는 원리를 이용하여 냉각관도 동일하게 식물의 뿌리가 성장하듯이 설치하여 목표했던 온도편차 값에 도달하기 전까진 냉각관도 세분화하는 방식으로 구현이 가능하도록 개발하였고 자동화된 프로그램으로 냉각회로 설계에 대한 명확한 방법론도 제시함.
- 최종적으로 본 연구에서 개발된 방법은 실제 자동차의 헤드 램프 렌즈 커버 제품에 적용하여 효율성을 검증함.

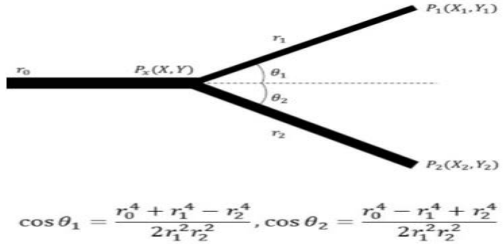

Fig. 1. Murray's Law

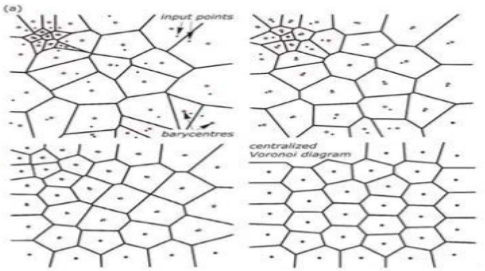

Fig. 2. Centroidal Voronoi Diagram

Fig. 3. Change of the circuit configuration through the evolution

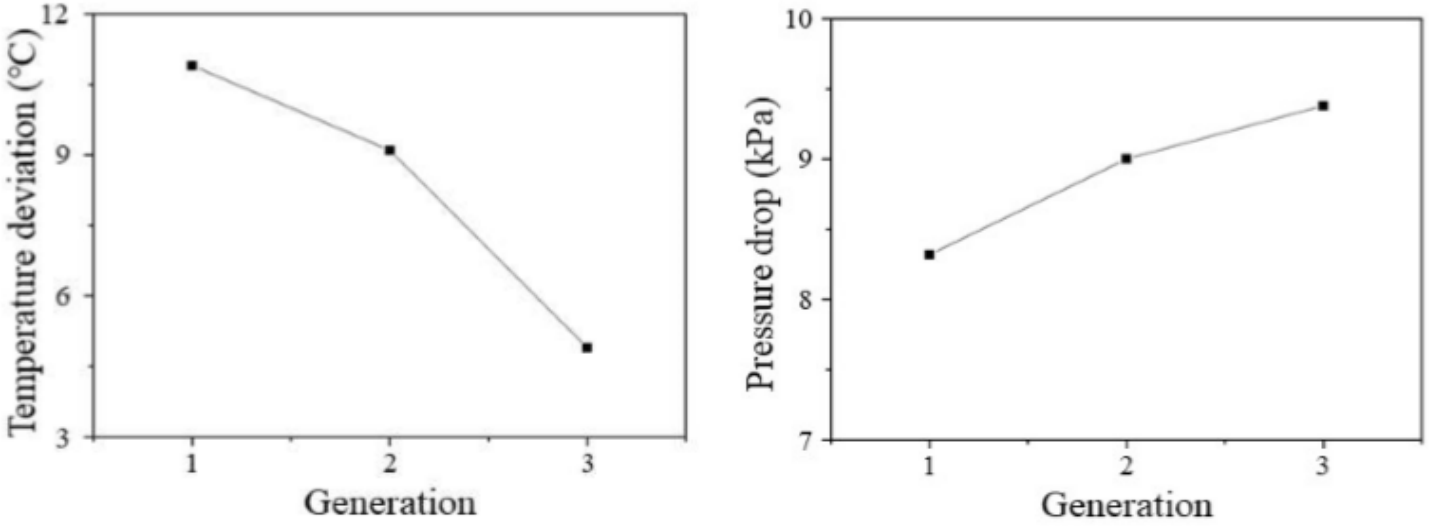

Fig. 4. Temperature deviation and pressure drop according to the generation

✓ Biomimetic engineering of conductive curli protein films[3]

- 펩타이드 및 단백질로부터 얻어진 생체 전자 시스템 (Bio-electronic systems)을 개발하는데 있어 유연성 (novel flexible), 생체 적합성 (biocompatible), 생물 활성 장치 (bioactive devices) 등이 중요하며 이러한 시스템은 자연적으로 발생하는 전기 활성 박테리아 (electro-active bacteria)의 단백질성 부속물 (protein-aceous appendages)을 모방하여 전자 수송을 디자인함.

- 방향족 잔류물 (aromatic residues) 함량이 높은 전도성 단백질에서 영감을 얻어 장거리 전자 수송이 가능한 대장균 박테리아가 생산하는 섬유질 섬유로 섬유질 단백질 지지체를 개발함.

- 이 논문은 single self-assembling CsgA curli subunits에 대한 다양한 컨텐트, spatial positioning의 정의, 방향족 잔류물을 포함하는 curli 섬유의 유전 공학 및 특성을 보고하고 있으며 새로운 기능을 가진 유전 공학 단백질인 CsgA 단백질의 다양성을 보여주고 있음.

- 천연 curli film과 비교하여 정제 과정을 거친 가공된 박막 curli film이 더 큰 전도성을 나타냈으며 거시적인 겔 및 필름의 제조 가능성을 입증함으로써 전도성 지지체 개발, 모델링, 단백질 공학 그리고 생합성 제조를 결합한 바이오 하이브리드 기술의 가능성을 제시함.

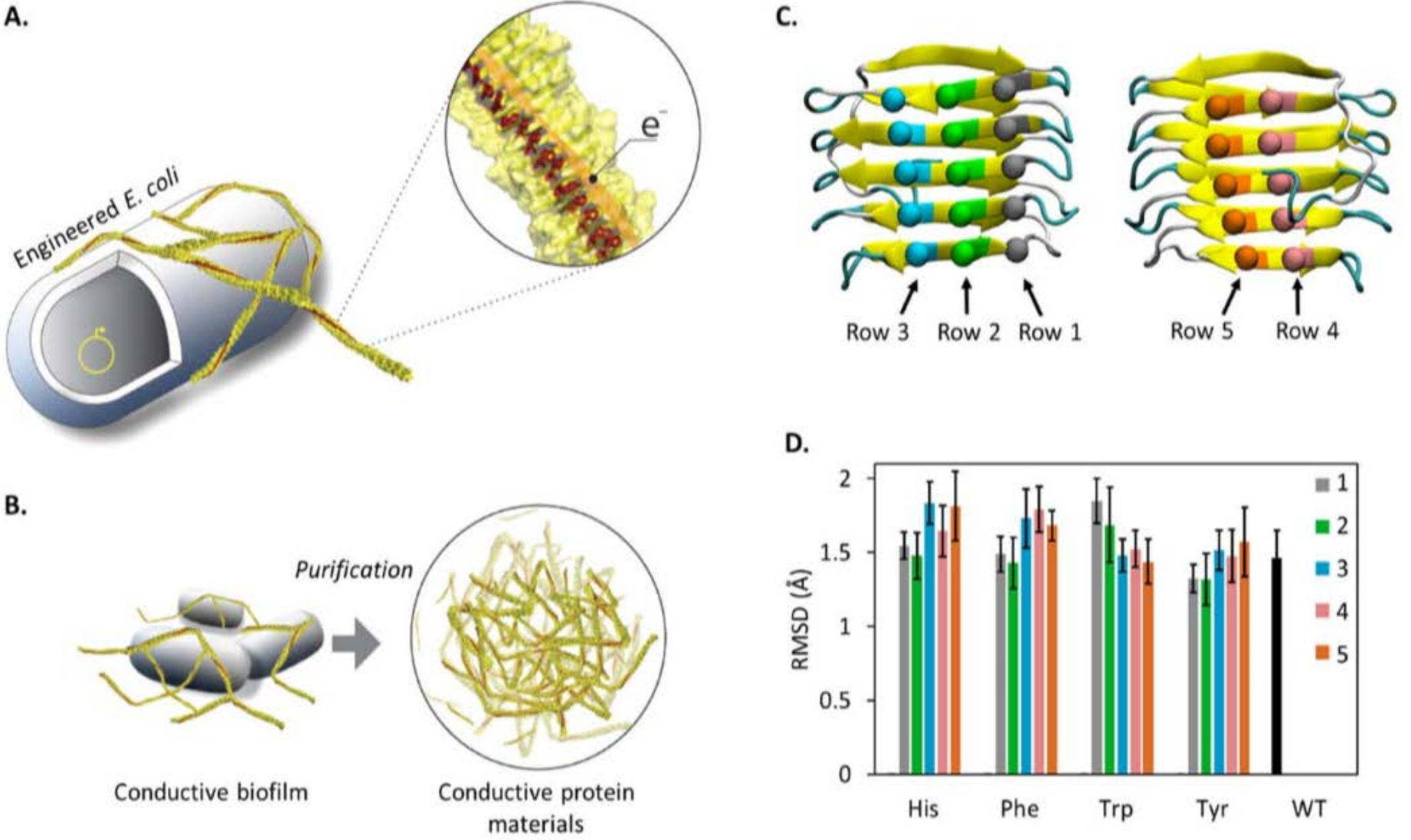

Figure 1. Engineering electronically conductive protein-based materials, based on electron transfer via densely-packed aromatic residues organized along self-assembling CsgA proteins. (A) Schematic depicting the production of mutant curli fibers containing aligned aromatic residues designed to mediate long-range electron transport. (B) Bacteria can be separated easily from conductive curli fibers via filtration to produce macroscopic conductive biomaterials composed of semi-purified curli fibers. (C) Positions of five arrays of aromatic residues (rows 1 through 5) to generate different aromatic CsgA variants. (D) RMSD values derived from molecular dynamics simulations for each aromatic CsgA mutant, as an indication of the stability of each mutant. Labels from 1 through 5 refer to the positions of the five rows of mutations shown in B. The stability of mutant fibers with different aromatic residues (His, Phe, Trp and Tyr) was simulated and compared with WT fibers (black bar). Because all RMSD values are below 2 Å, we concluded that the mutations would not disrupt the CsgA structure.

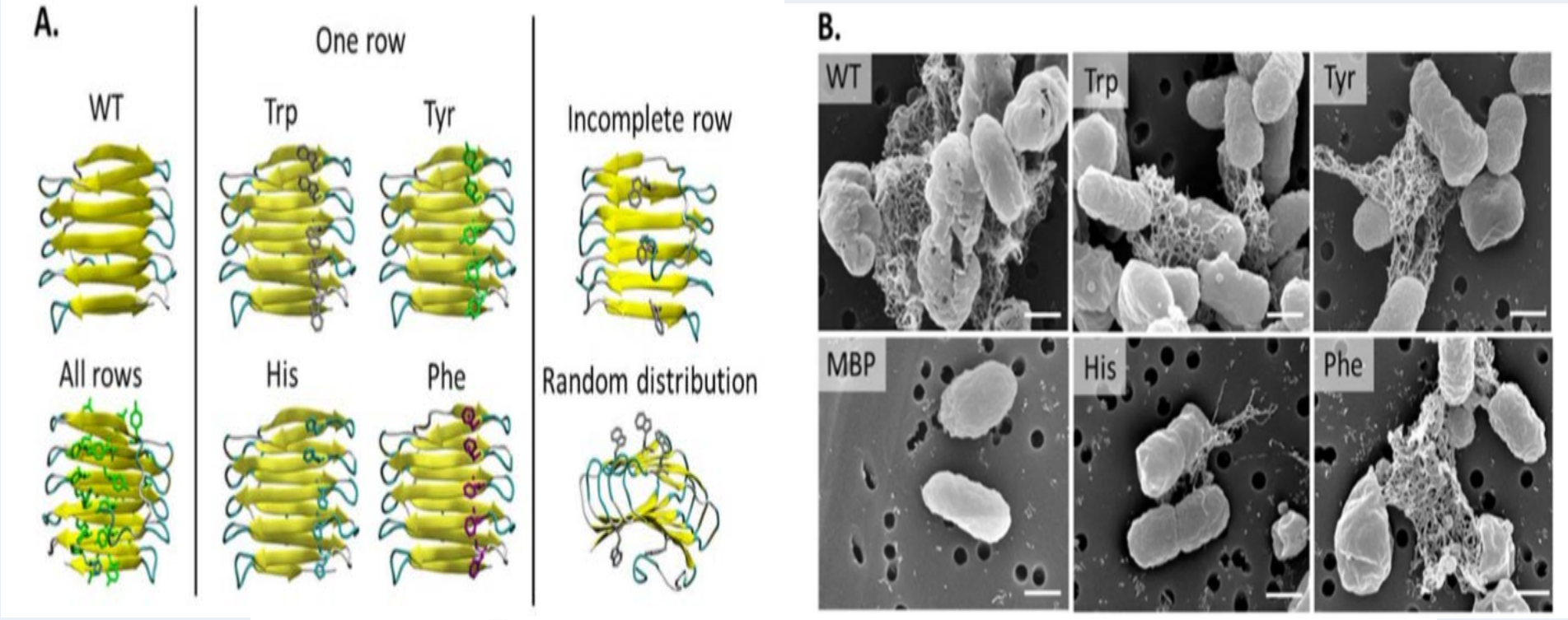

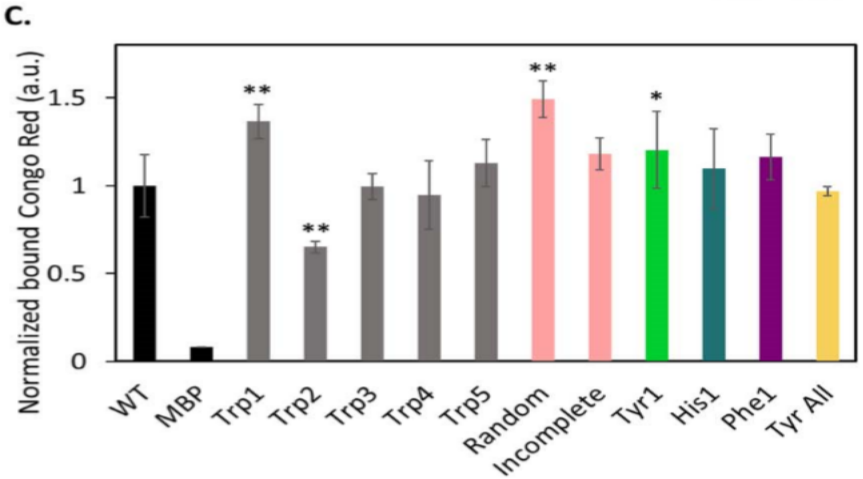

Figure 2. Expression and morphology of a library of aromatic CsgA mutants, revealing the formation of amyloid fibers. (A) Computationally-derived models of CsgA bearing various aromatic residue mutations. Residues were organized as one or multiple rows on the surface of CsgA, or as an incomplete row or random distribution. (B) Bacterial cells expressing curli fiber variants with aromatic residue mutations in row 1, imaged by SEM. Scale bars: 500 nm. (C) Congo red binding assay for bacteria expressing aromatic mutant curli fibers. Normalized bound Congo Red is a measure of this amyloid-specific dye bound to bacteria-curli fiber pellets, obtained by measuring free dye in solution and subtracting from total dye signal. Bacteria expressing WT CsgA or maltose-binding protein (MBP) were used as controls. Error bars represent standard deviation from the mean. Student's t-tests indicate significant differences in Congo Red binding between every curli fiber type and MBP ($p < 0.01$). T-tests comparing mutant fibers with WT fibers: * ($p < 0.1$), ** ($p < 0.05$).

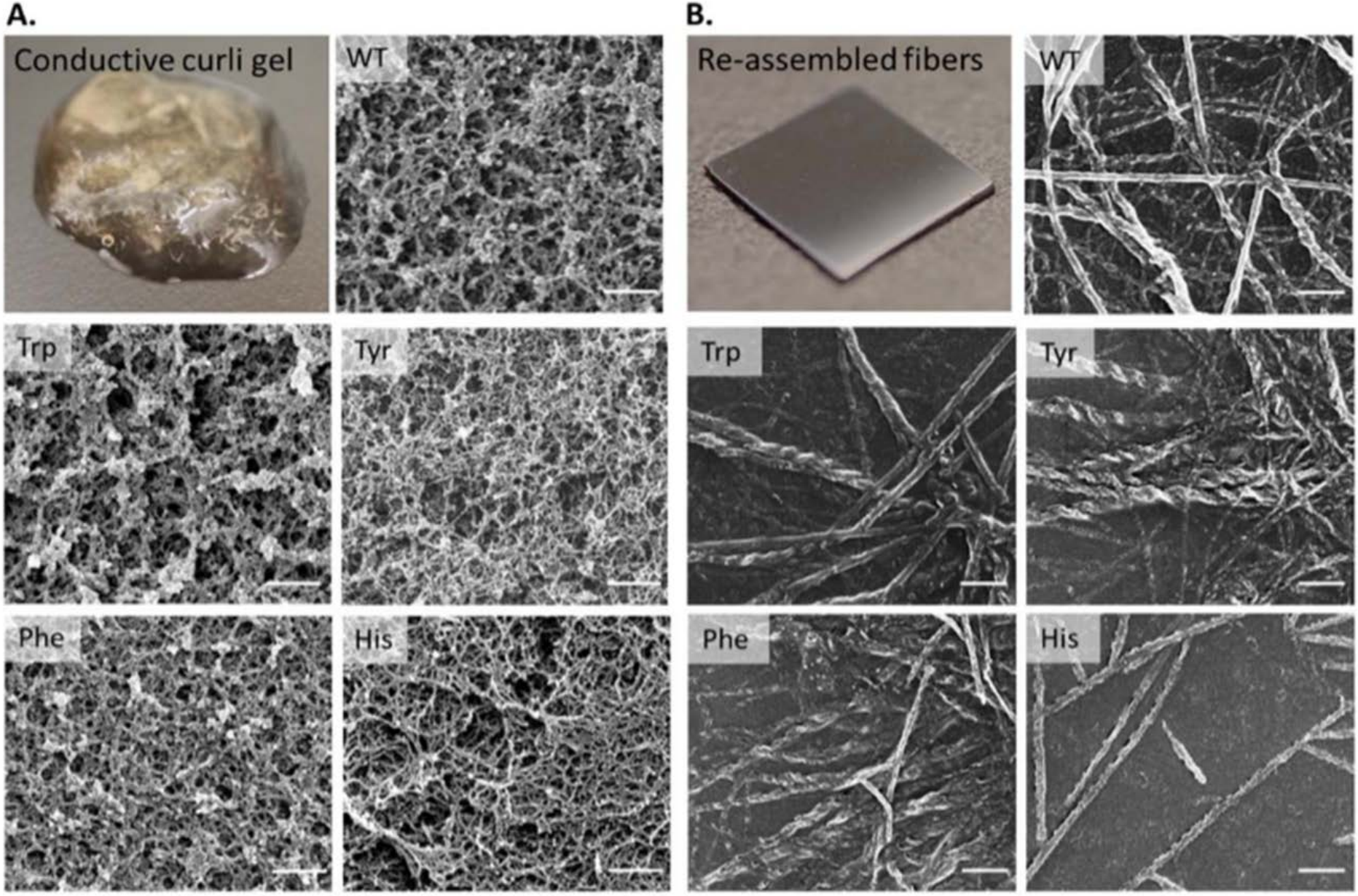

Figure 3. Protein gels or single fibers obtained from aromatic CsgA mutants. (A) Protein gels as obtained directly after vacuum filtration purification of curli fibers from bacterial culture. SEM images were taken after critical point drying to maintain the hydrated gel morphologies. Scale bars: 500 nm. (B) Protein fibers on silicon substrates obtained after disassembling and re-assembling protein gels. SEM images were taken for dried reassembled fibers. Scale bars: 500 nm.

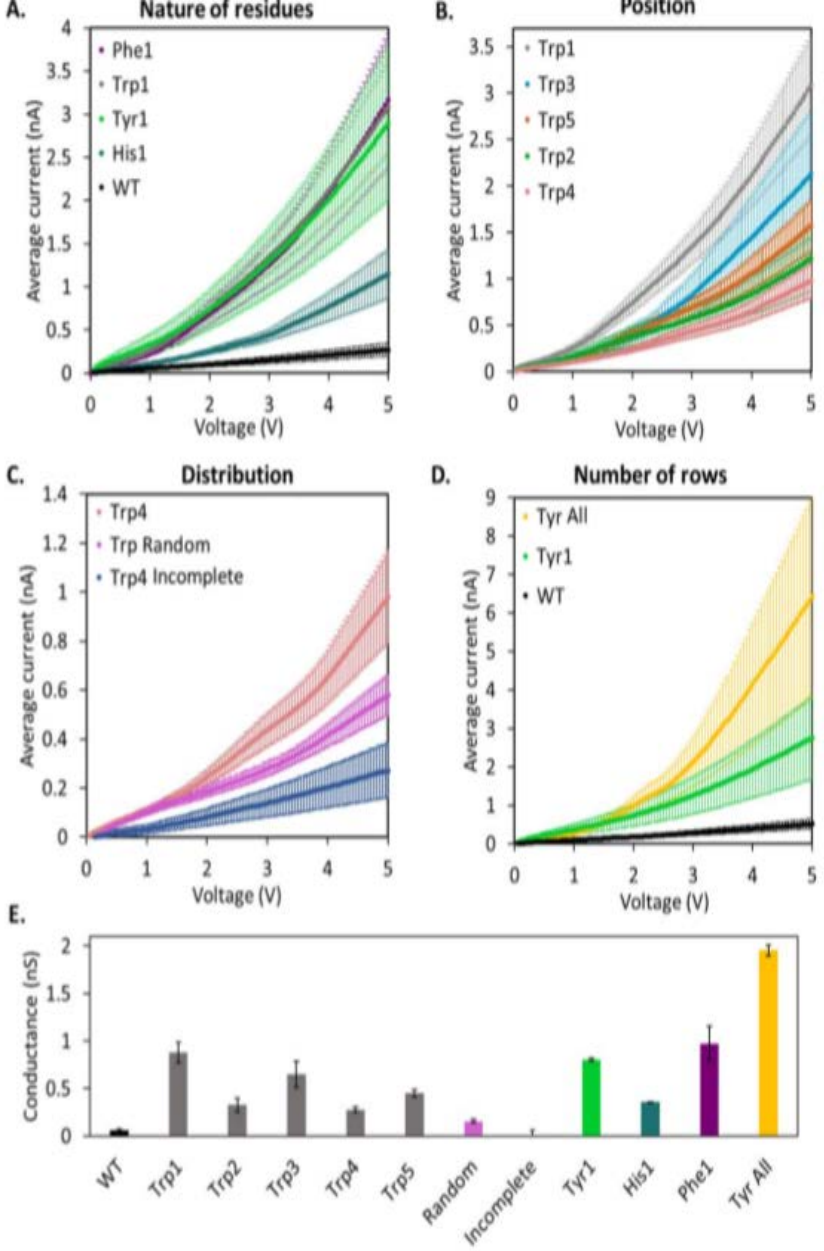

Figure 4. Current–voltage characteristics of aromatic CsgA mutant thin films. Average current–voltage response for mutant proteins deposited on electrodes with 20 μm spacing, for (A) different aromatic residues in row 1, (B) five different positional arrays of Trp residues, (C) Trp mutations arranged in either a contiguous row, an incomplete row or randomly on the CsgA surface, and (D) Tyr mutations in row 1 or in all five rows simultaneously, compared with WT fibers. (E) Conductance of aromatic mutant CsgA films calculated from the slope of each current–voltage curve between 3 and 5 V. For (A) through (D), error bars on individual data points represent standard deviation from the mean ($n \geq 3$). For (E), error bars were derived from the maximum error on the slope of the current–voltage curves. For (A) through (D), legends list samples in order, from protein films yielding the highest to the lowest current at 5 V.

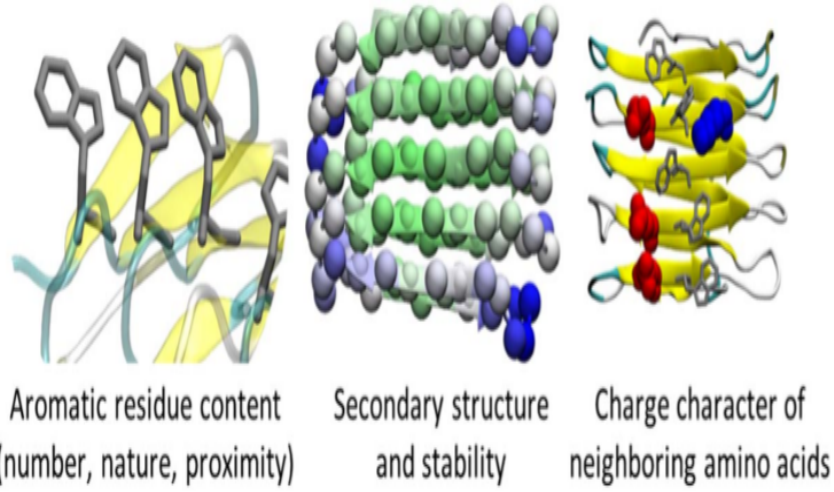

Figure 5. Proposed factors affecting the conductance of CsgA thin films. Design considerations for optimal conductance include the content and positioning of aromatic amino acids (*left*), the location of mutations within β-sheets with low mobility (*middle*), and the presence of fewer charged neighboring residues (*right*). The middle CsgA is colored by RMSF, with the lowest values in green and highest values in blue and α-carbons shown. Charged residues neighboring row 2 are shown at the right, with (−) charges in red, and (+) charges in blue.

✓ Surface Engineered Biomimetic Inks Based on UV Cross-Linkable Wood Biopolymers for 3D Printin[4]

- 나노셀룰로오즈 (nanocelluloses)는 extra-cellular matrix와 유사한 기계적 강도, 구조를 가지고 있어 다양한 조직 모방체를 제조하기 위한 3D 바이오 프린팅의 새로운 생체 물질로 보고되고 있음.

- 셀룰로오즈 나노 섬유 (cellulose nano-fibrils, CNF)와 가교 결합이 가능한 헤미셀룰로오즈 유도체 (cross-linkable hemi-cellulose derivatives)를 기반으로 UV-aided extrusion printing이 가능한 생체 모방 잉크 개발을 보고함.

- Extrusion-based 3D printing 기반 생체 모방 잉크인 UV cross-linkable galacto-glucomannan methacrylates (GGMMAs)는 GGMMA의 치환 및 GGMMA와 CNF 사이의 조성비의 변화에 따라 2.5 ~ 22.5 kPa의 폭넓은 하이드로 겔의 기계적 특성을 보고함.

- CNF/GGMMA 잉크로 인쇄된 지지체는 인간 피부 섬유아 세포 (human dermal fibroblasts)와 췌장 종양 세포 (pancreatic tumor cell)에 적용해 봤을 때 우수한 세포 적합성, 지지체의 부착성, 세포 증식을 입증함.

- CNF/GGMMA 잉크는 조직 공학 (tissue engineering), 암 세포 연구 (cancer cell research), 그리고 고효율 약물 스크리닝 (high-throughput drug screening) 연구 분야에서 세포 매트릭스 (cell−matrix)로 세포-세포 상호 작용 연구 (cell−cell interaction studies)에서 요구하는 새로운 3D 프린팅 바이오 잉크로서 개발됨을 보고함.

Scheme 1. Illustration of the Chemical Structures of GGMMA and GGM

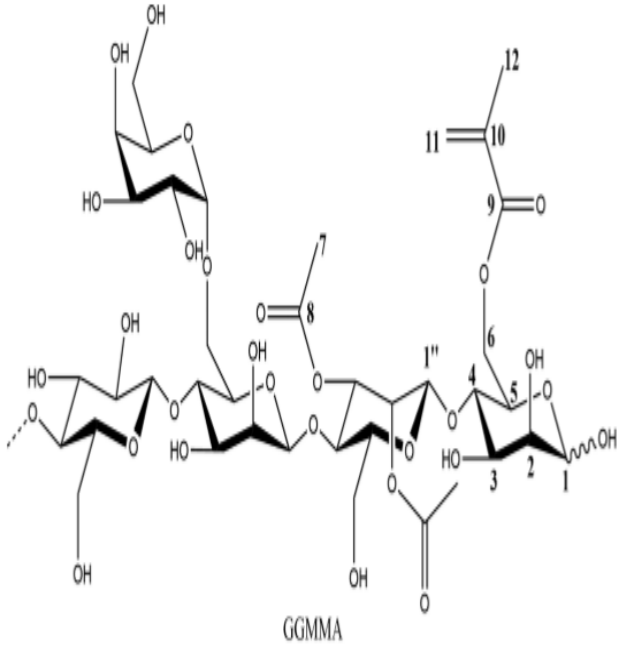

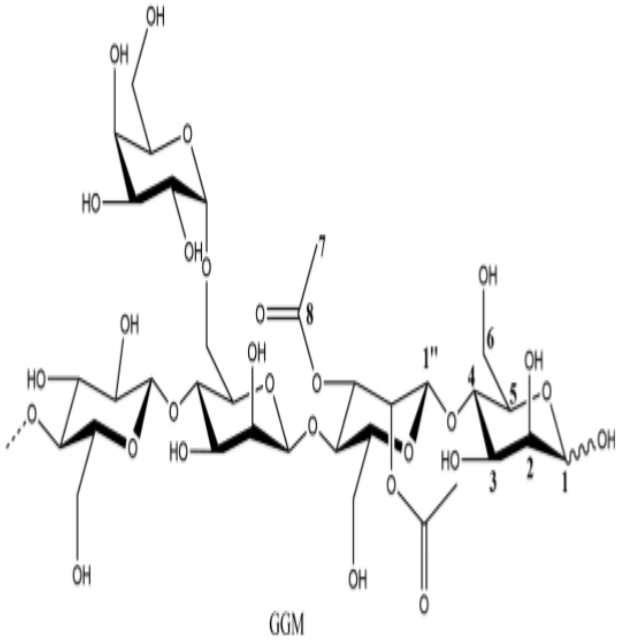

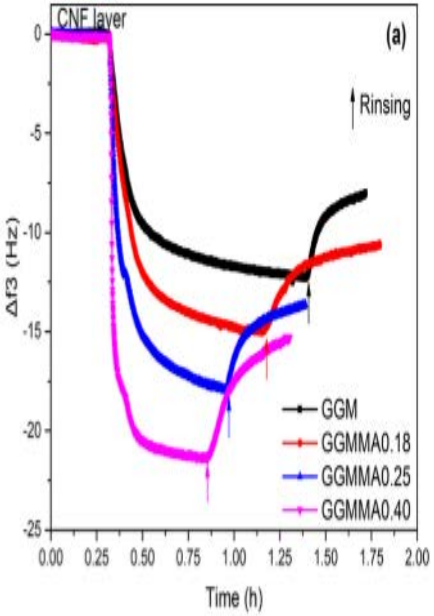

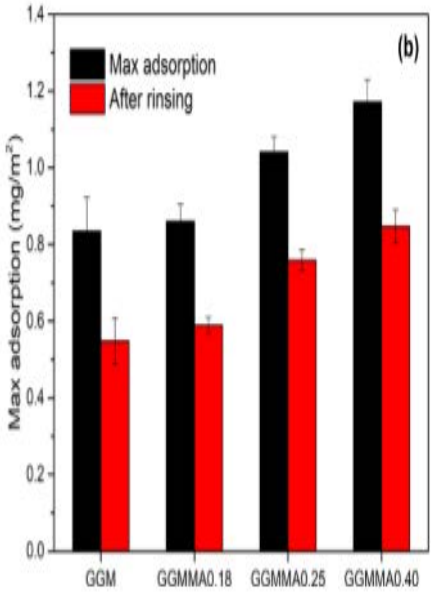

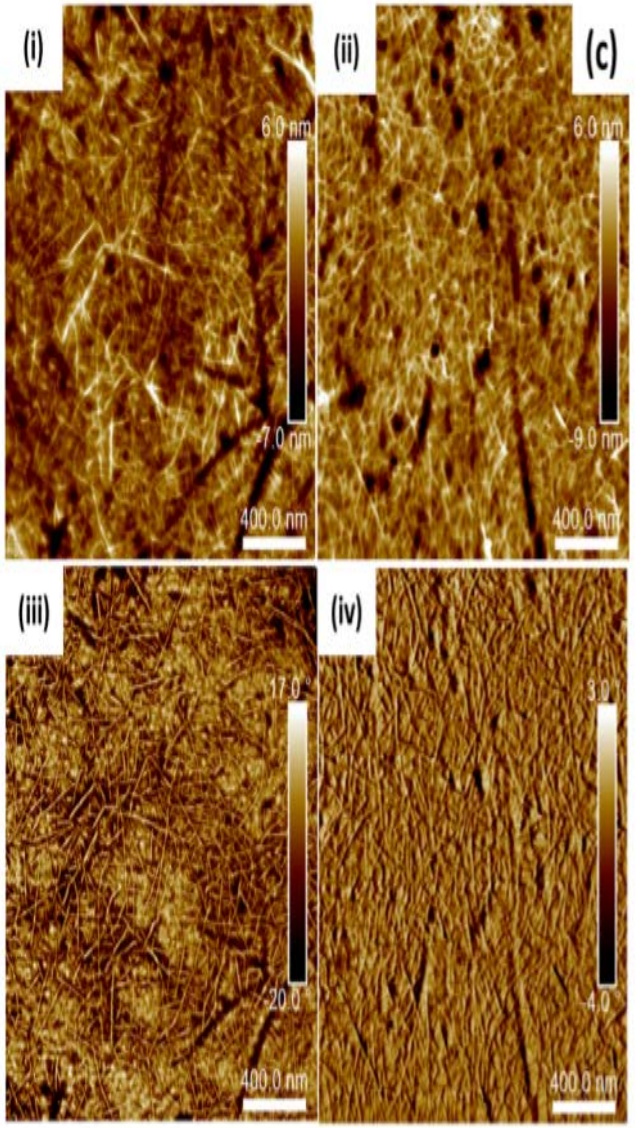

Figure 2. (a) QCM-D adsorption curve of GGMMA onto the CNF layer; (b) adsorbed GGMMA mass on the CNF layer; and (c) AFM images of CNFs in the height mode (i) and phase mode (iii) and of GGMMA0.40 on the CNF layer in the height mode (ii) and phase mode (iv) with a scale bar of 400 nm.

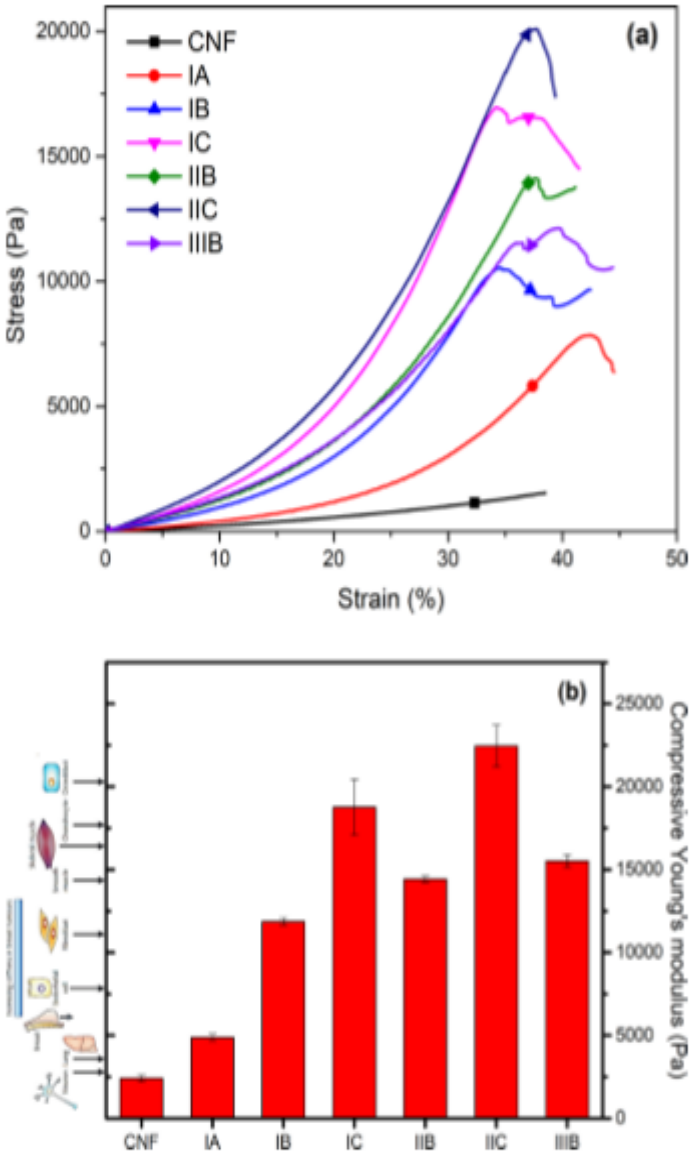

Figure 4. Compressive stress–strain profiles of the cast disc with different ink formulations (a) and their compressive Young's moduli (b). (Cell image was reproduced with permission from Springer Nature).

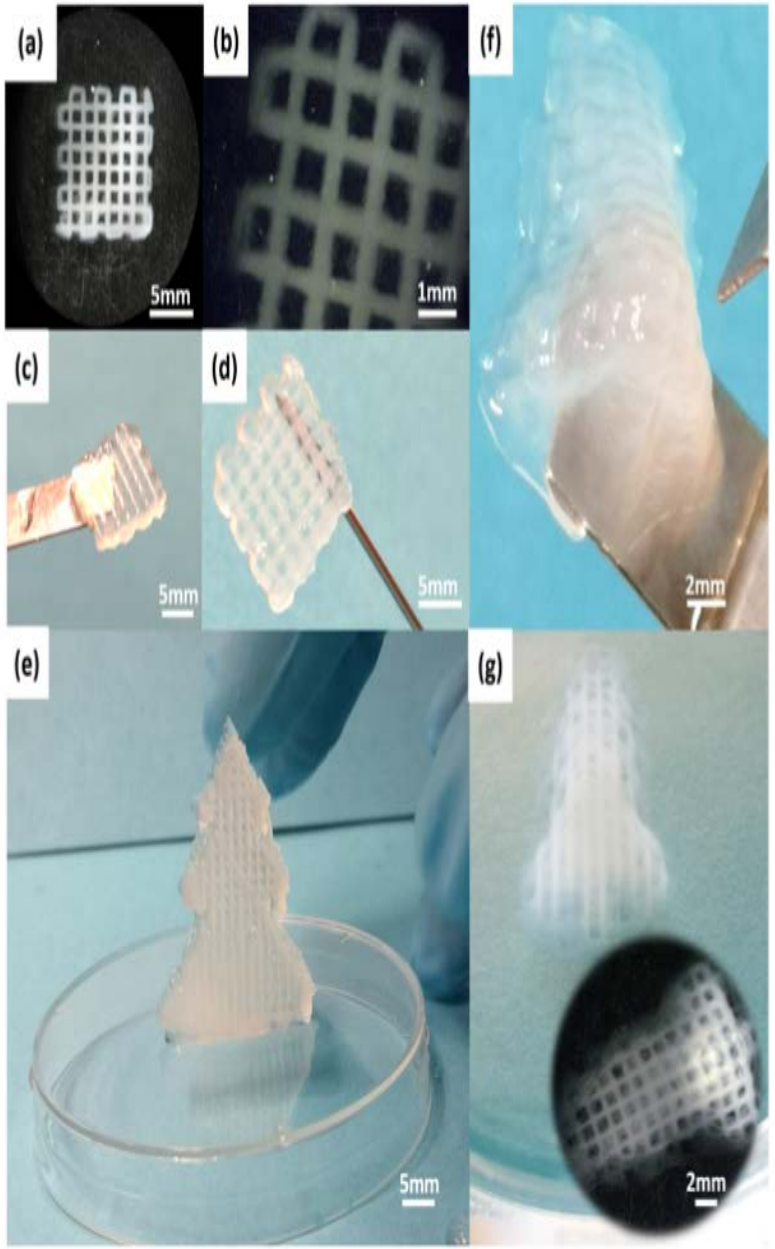

Figure 5. Scaffold with high resolution was printed with ink IA after UV cross-linking (a–d). Top view (a), edge view (b), handling with spatula (c), and holding with needle (d) of the printed scaffold with dimension of 10 mm × 10 mm × 2 mm. Standing printed and cross-linked spruce tree model with ink IIB (e). Printed and cross-linked nose model with inner structure in high resolution by ink IA (f) and (g).

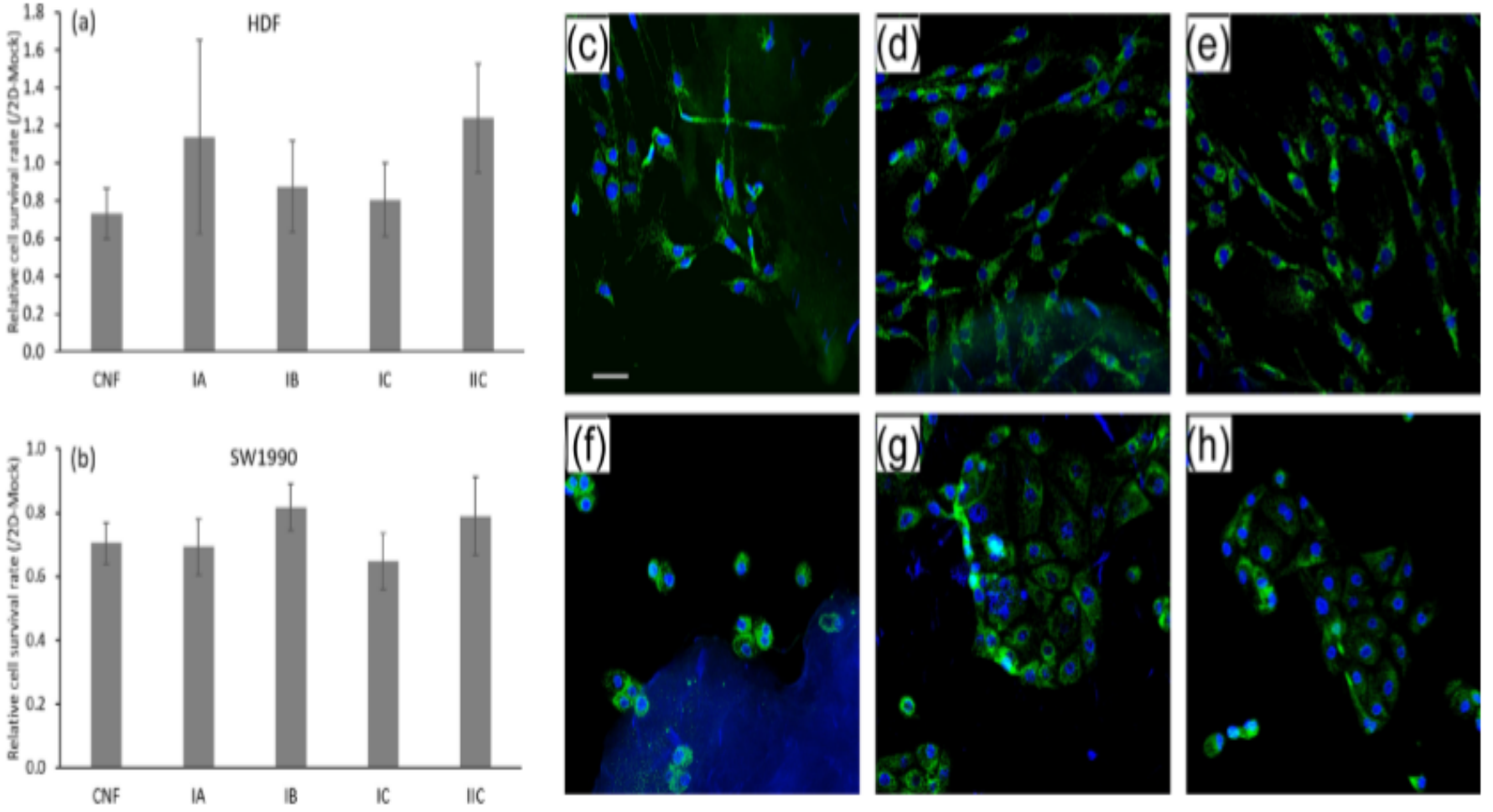

Figure 6. Cell survival rates on the seeding matrices printed with various inks were measured for HDF (a) and for SW-1990 (b) after 48 h of incubation at a density of 5×10^3 cells/96-well by using the MTT assay; bar = mean ± STDEV and $n = 3$. Representative confocal images of the cells were recorded after 48 of incubation for HDF in the 3D matrix of CNFs (c), ink IB (d), and ink IC (e) and for SW-1990 in the 3D matrix of CNFs (f), ink IB (g), and ink IC (h). The cell morphology is shown by phalloidin (green), and nuclei were counterstained by DAPI (blue). Scale bar: 50 μm.

✓ Biomimetic Peptide Nanowires Designed for Conductivity[5]

- 유기화합물을 환원시켜 전기를 생성하는 박테리아 Geobacter Sulfurreducens에 의해 생성된 섬유질 펩타이드 기반 나노 와이어 (wire)는 탁월한 전도성을 나타냄. 이 박테리아의 전도 메커니즘은 밀접하게 조정된 방향족 아미노산과 hopping/charge transfer를 통한 전자들의 조합에 인한 것으로 알려짐.

- 박테리아의 나노 와이어를 형성하는 단백질은 coiled-coil로 구성되어 있는데, 이런 구조에 따라 합성된 펩타이드는 aromatic residues의 혼입하여 펩타이드 섬유의 전도성이 향상되는 생체 모방 시스템을 사용하는 것을 알게 됨. 이러한 펩타이드 서열의 de novo desig은 펩타이드 겔의 전도성을 향상시키는데 사용됨.

- 본 연구는 aromatic residues가 펩타이드 겔의 전도성에 기여함을 입증하였으며 펩타이드 서열 확인과 fibril assembly를 실험한 결과 펩타이드 기반 전도성 나노 와이어 개발이 bio-electronic과 bio-energy 응용 분야에서의 활용 가능성이 있음을 보고함.

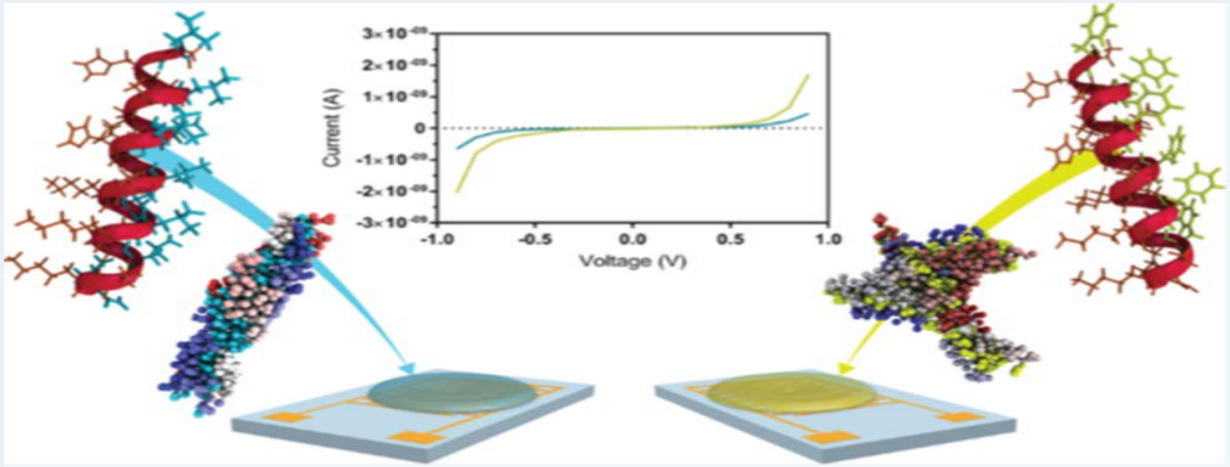

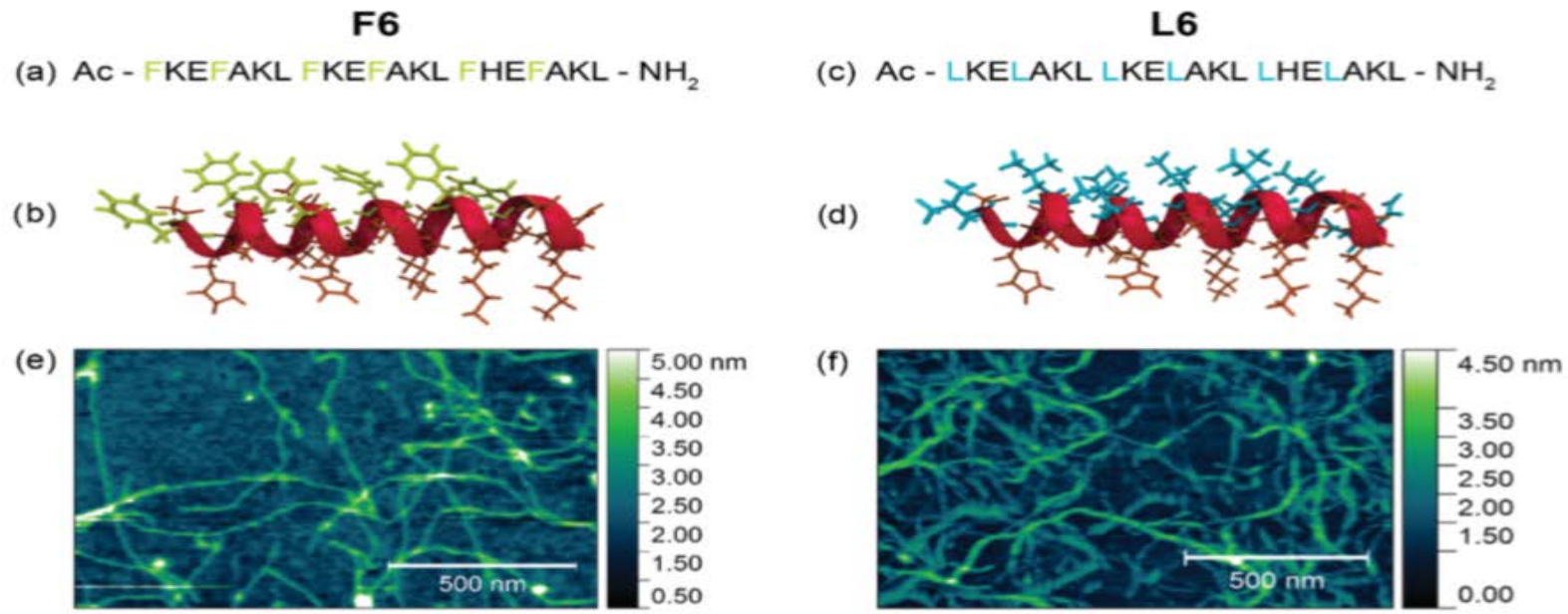

Figure 1. Amino acid sequence (a, c), secondary structure representation showing side chains (b, d), and atomic force microscopy (AFM) topography images for F6 (e) and L6 (f). Scale bars on AFM images: 500 nm (x) and 4.5 nm (z).

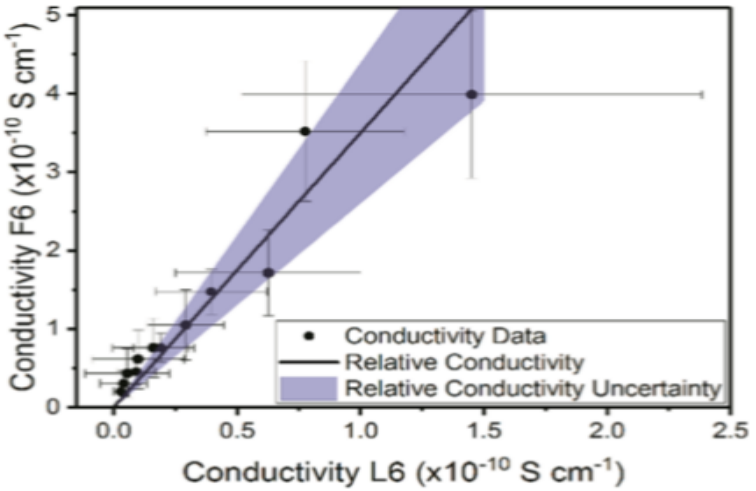

Figure 3. Ratio of the voltage-dependent conductivities between F6 and L6 peptide films. The data indicates a consistent ratio as a function of voltage across the entire voltage range, though noting that the uncertainty increases for smaller values of voltage. The solid line indicates the weighted mean value, and the shaded area indicates the uncertainty around the mean. Corresponding values are 3.5 ± 0.9 (2SE), indicating that F6 is indeed more conductive than L6.

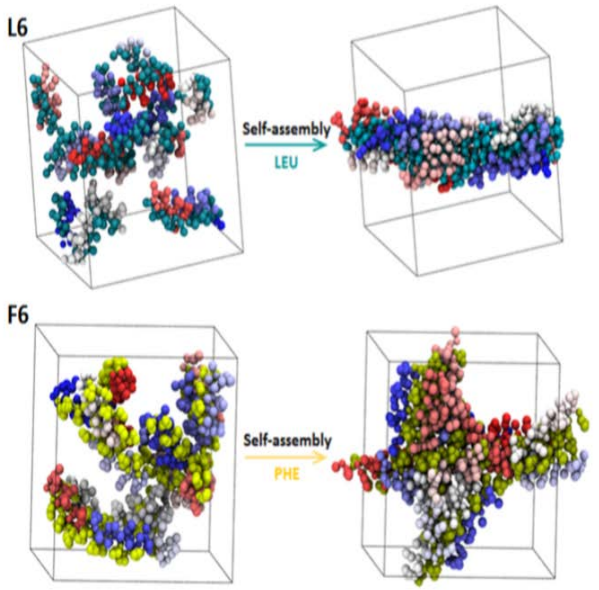

Figure 6. Self-assembly of L6 (above) and F6 (below) into nanofibrils as obtained from MD simulations using the coarse-grained MARTINI model for the peptides. On the left are snapshots of L6 and F6 peptides randomly distributed inside simulation boxes with leucine and phenylalanine shown in green and yellow, respectively, and different peptide chains presented in different colors. On the right, after 10 μs simulation, L6 has assembled into a nanofibril with moment of inertia (MOI) along the principal axes of the largest cluster of 7.74, whereas F6 has assembled into a higher dimension nanofibril with MOI of 2.23.

✓ Advances in biomimetic stimuli responsive soft grippers[6]

- 지능형 액츄에이터(intelligent actuators), 센서 또는 생체의학 도구(bio-medical tool)로 활용할 수 있는 다양한 생체 모방 자극 반응형 소프트 그리퍼 (biomimetic stimuli responsive soft gripper)로써, N-iso-propyl acrylamide hydrogel, 열 및 광 반응성 액정, pneumatic driven shape-morphing elastomer로 구성된 자극-응답 그리퍼에 대한 연구 진행을 보고함.

- 자극에 반응하는 부드러운 그리퍼를 만들기 위해 포토 리소그래피 및 직접 프린팅 방식과 같은 high-throughput assembly methods에 대해 기술함.

- 이 리뷰는 tethered/untethered multi scale smart soft actuators, manipulators, 또는 bio-medical devices로써 활용될 수 있는 stimuli-responsive soft gripping robot 연구에 중점을 두고 있음.

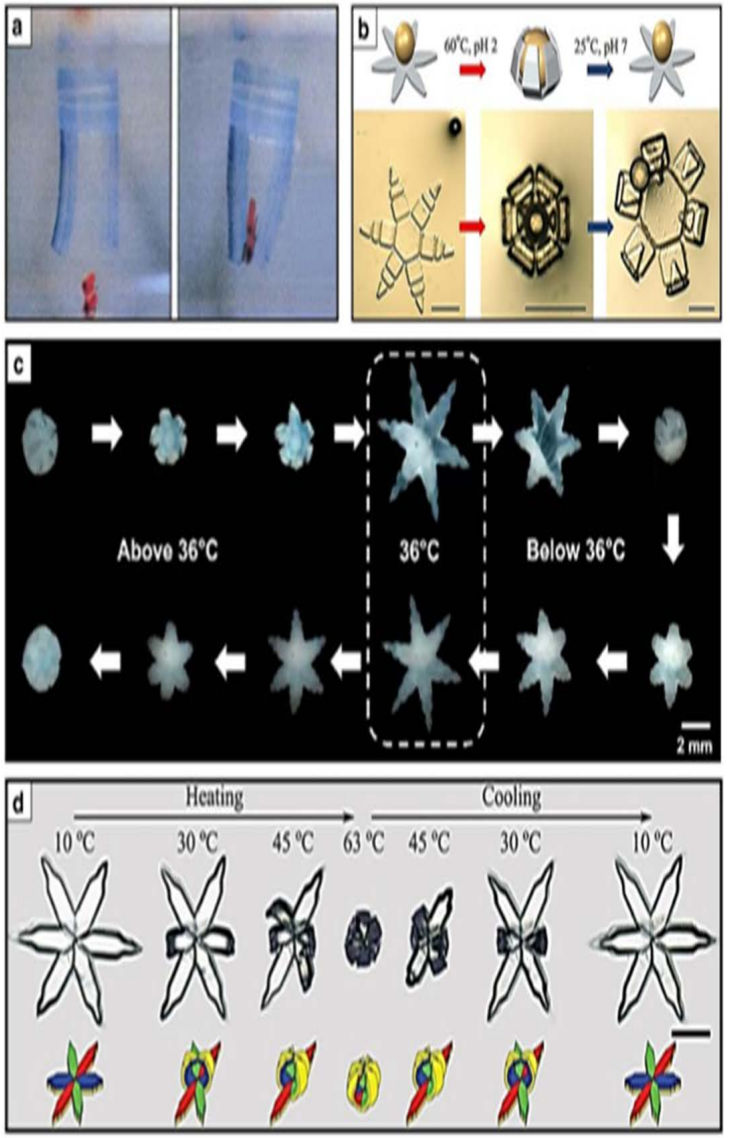

Fig. 1 Biomimetic soft gripping robots composed of stimuli responsive hydrogels, polymer, or hybrid combination of them. **a** *N*-isopropylacrylamide (NIPAM)-modulated thermal responsive bigel stripped grippers (reproduced with permission [17]. Copyright 1995, AAAS). **b** Poly(*N*-isopropylacrylamide-acrylic acid)(pNIPAM-AAc) soft gripper that reversibly actuates when triggered by temperature or pH (reproduced with permission [13]. Copyright 2014, IOP Publishing). **c** Thermally responsive self-folding bilayer soft gripper that closes and opens reversibly when passing by LCST at 36 °C (reproduced with permission [9]. Copyright 2015 American Chemical Society). **d** Reversible four-state shape changes of soft grippers during heating and cooling process (reproduced with permission [26]. Copyright 2018 Wiley-VCH)

➢ Material selection
- N-isopropylacrylamide (NIPAM)-based stimuli-responsive hydrogels

- 자극 반응 물질은 열 (전기, 광열), pH, 자기장, 빛 및 생화학 효소와 같은 외부 자극에 반응하여 화학적 및 물리적 특성을 변화시키는 물질임.

- 대부분의 자극 반응 물질은 일반적으로 단일 겔 네트워크에서 친수성(예 : 아미드 및 카르 복실) 및 소수성(즉, 메틸, 에틸 및 프로필) 그룹이 결합하여 합성되었으며 이렇게 합성되어진 복합 겔 네트워크 설계는 겔 시스템에서 고유한 특성 변화를 나타내는 낮은 임계 용액 온도 (LCST)에 따라 변화하는 특성을 가짐. LCST 아래에선, 복합 겔 시스템은 물을 흡수하여 친수성 특성을 보이고, LCST 위에선 소수성 특성이 우세해지고 수분 탈착을 초래함.

- NIPAM은 중요한 자극성 LCST 하이드로 겔 중 하나이며 LCST 위의 온도에선 NIPAM 기반 하이드로 겔은 소수성 (de-swollen)을 나타내며 32 ~ 36 ℃의 LCST 아래에선 친수성 팽창의 특징을 가짐. LCST를 기준으로 온도가 달라짐에 따라 나타내는 swelling/de-swelling mechanism은 외부 자극에 노출 될 때 NIPAM 기반 하이드로 겔의 특성이 달라져 모양이 변화하기 때문에 광범위한 응용이 가능해짐.

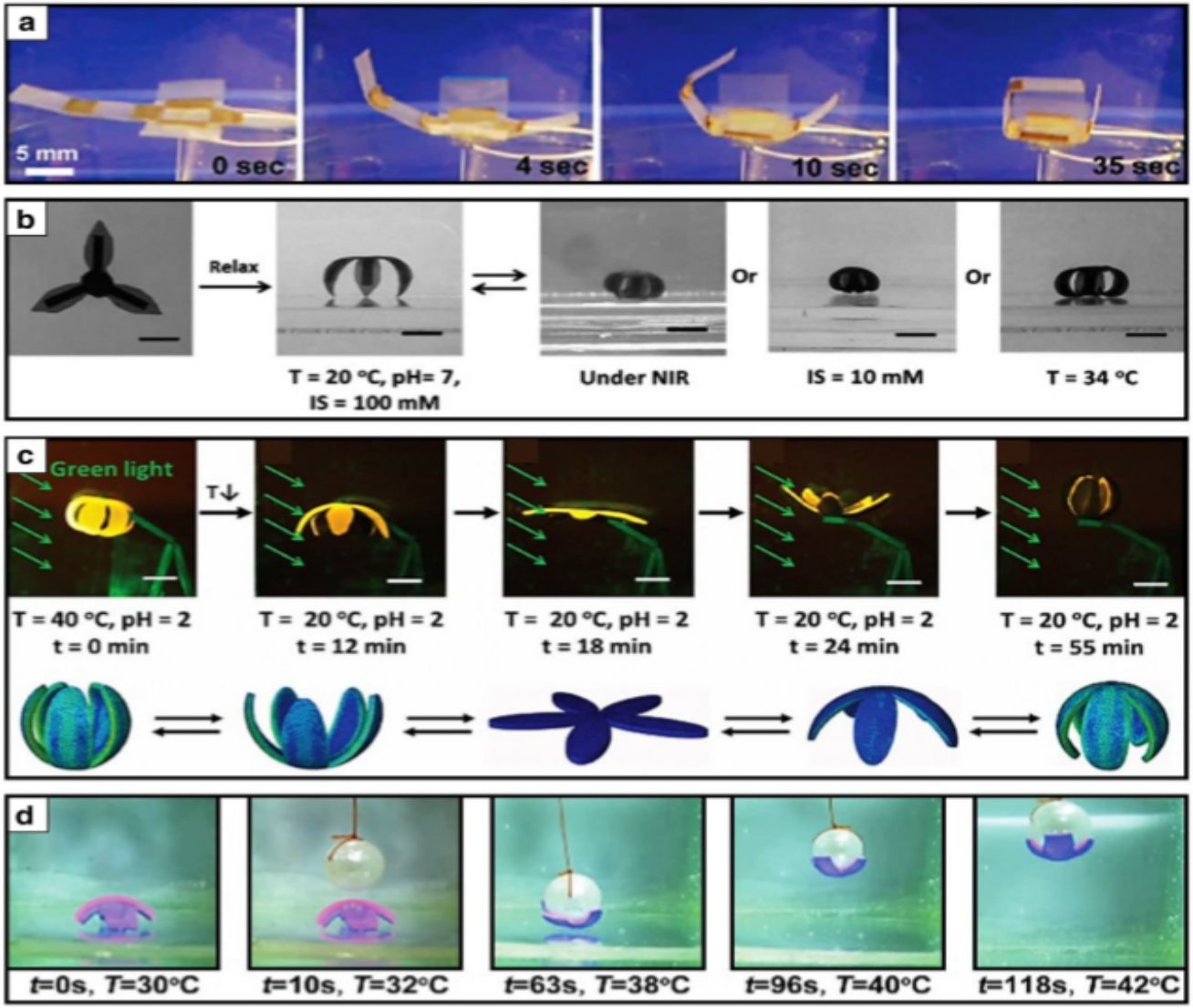

Fig. 2 Biomimetic stimuli responsive soft grippers composed of poly *N*-isopropylacrylamide (pNIPAM) based hydrogels hybridized with nanoparticles. **a** Programmable folding cube composed of single-walled carbon nanotube (SWNT)-pNIPAM and low-density polyethylene (LDPE) bilayer that actuates reversibly in water (reproduced with permission [66]. Copyright 2011, American Chemical Society). **b** Multi near-infrared light (NIR), ionic strength (IS), and temperature change responsive soft gripper composed of graphene oxide (GO)-pNIPAM and pNIPAM-poly(methylacrylic acid)(PMAA) bilayer (reproduced with permission [65]. Copyright 2016, Wiley–VCH). **c** Thermoresponsive biomimetic flower shaped fluorescent color displaying soft gripper composed of graphene oxide (GO)-pNIPAM and pH responsive perylene bisimide-functionalized hyperbranched polyethylenimine (PBI-HPEI) hybrid bilayer (reproduced with permission [68]. Copyright 2017, Wiley–VCH). **d** Temperature-controlled pNIPAM/pNIPAM-co-clay nanocomposite bilayer hydrogel gripper that grips a moving pearl (reproduced with permission [22]. Copyright 2015, Wiley–VCH)

- Liquid crystalline material-based stimuli-responsive hydrogels

- 액정 엘라스토머 (LCE) 및 액정 네트워크 (LCN)와 같은 액정 물질(Liquid crystalline materials)은 외부자극에 의해 모양의 변화가 생기는 물질임. LCE와 LCN은 일반적으로 유리 전이 온도 (Tg)와 기계적 특성에 따라 분류 될 수 있는데 LCE는 MPa 정도의 온도에서 실온보다 낮은 Tg를 나타내는 반면, LCN은 탄성 계수를 갖는 높은 Tg를 갖고 있음. 따라서, LCN/LCE 하이브리드는 분자의 정렬과 가교 정도를 조절하여 형상 기억 거동을 구체적으로 나타낼 수 있으며, 외부 자극에 노출된 후 굽힘, 비틀림, 회전 또는 접힘과 같은 가역적 형상 변화를 일으킴.

- 반응 형 액정 기반 스마트 소프트 그리핑 로봇 (responsive liquid crystalline-based smart soft gripping robot)은 액정 재료의 광 정렬 특성을 기반으로 개발되었으며 다양한 연구가 보고되고 있음.

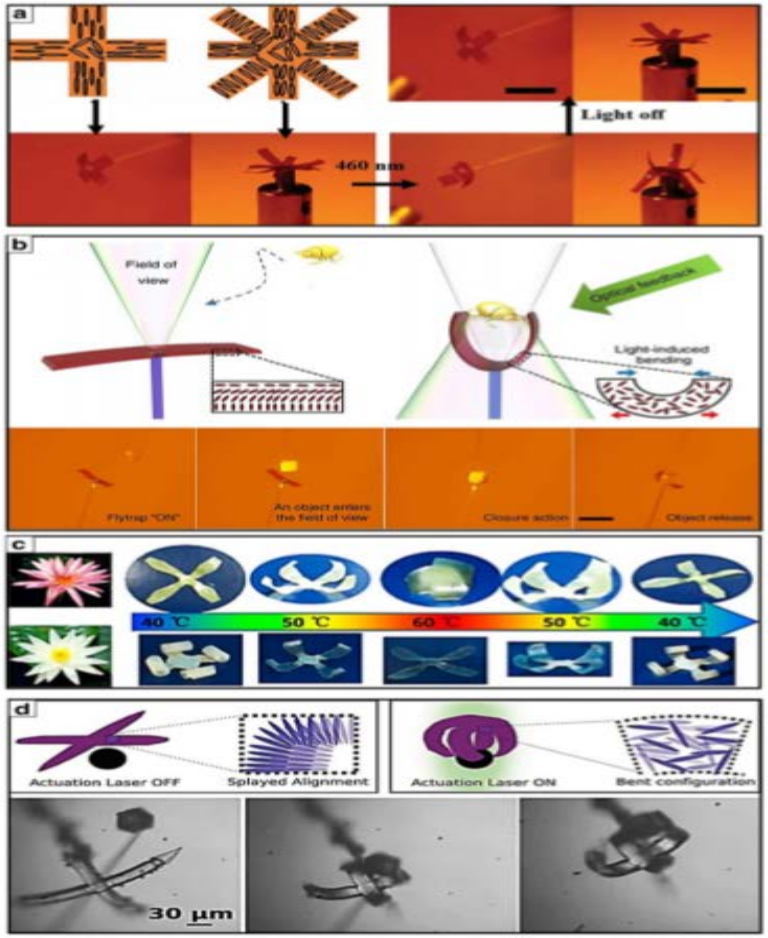

Fig. 3 Photothermal responsive liquid crystalline networks (LCNs) and liquid crystalline elastomers (LCEs) soft grippers. **a** Photothermal actuation of 4- or 8-armed soft grippers when exposed to 460 nm illumination that are composed of splay- or – 90° twisted nematic alignment patterns in a liquid crystal polymer networks film (reproduced with permission [75]. Copyright 2017, Wiley-VCH). **b** Flytrap mimetic light responsive self-folding liquid crystal elastomers (LCEs) gripper that captures an object according to light illumination intensity feedback (reproduced with permission [76]. Adapted with permission under the terms of the Creative Commons Attribution Non Commercial License 4.0 license. Copyright 2017, The Authors). **c** Water Lily flower mimicked thermoresponsive soft liquid crystal networks (LCNs) grippers that can open and close via induced smetic–nematic phase transition in LCNs according to heating and cooling process (reproduced with permission [7]. Copyright 2018, American Chemical Society). **d** Light driven actuation of LCNs soft grippers controlled by the mesogen alignment change (reproduced with permission [28]. Copyright 2017, Wiley-VCH)

➢ Methodology: Photolithography or 3D printing

- 자극에 반응하는 3D 장치 (stimuli-responsive 3D devices)를 제작하는 방법으로 직접 수동 조립 (direct manual assembly), 인쇄 (printing), 성형 (molding), 하향식 리소그래피 (top–down lithography), 매크로부터 나노 스케일까지의 상향식 합성 (bottom–up synthesis) 등 다양한 방법들이 보고되고 있음.

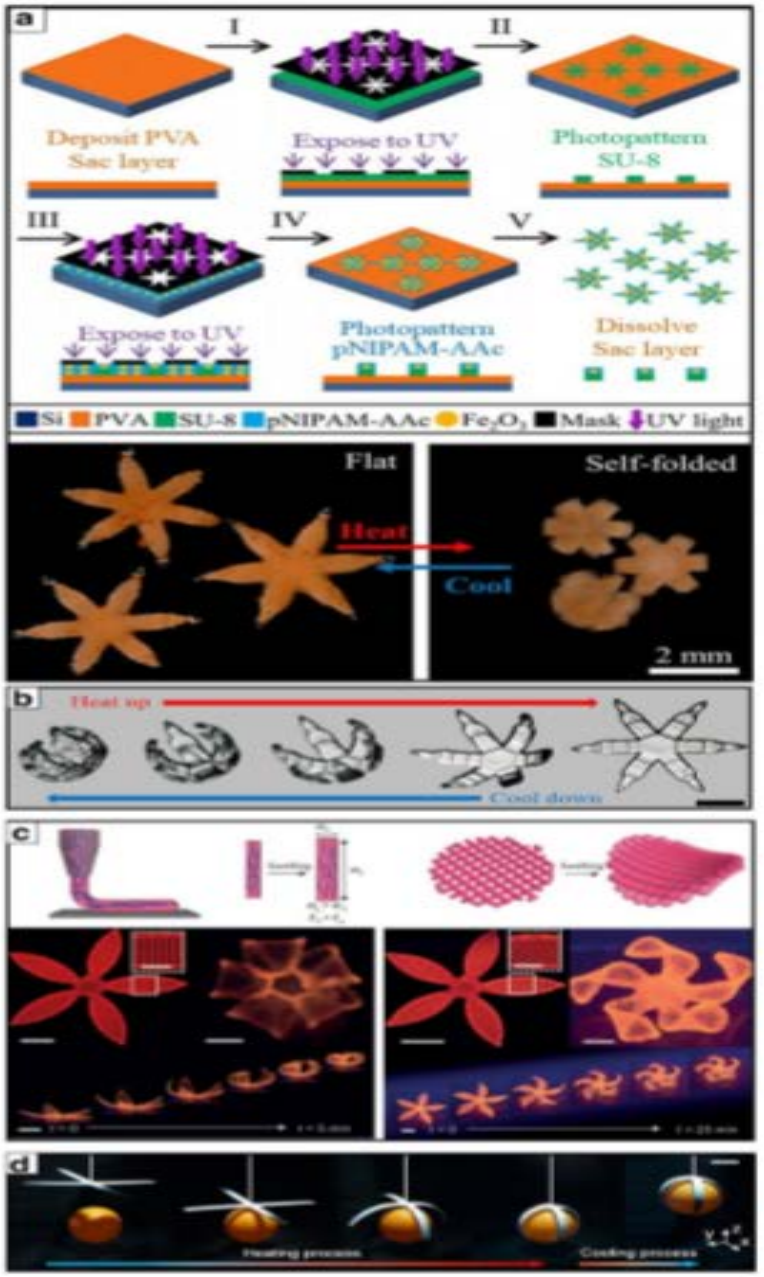

Fig. 4 Two main photolithographic and 3D printing methods to fabricate stimuli responsive soft grippers. **a** Process flow of photolithography to create stimuli responsive soft grippers with following two-step UV exposures. The photopatterned bilayer soft grippers that close on heating and open up on cooling reversibly (reproduced with permission [79]. Copyright 2018, IEEE). **b** Photolithographically patterned biodegradable soft grippers that respond to temperature change (reproduced with permission [83]. Copyright 2019, American Chemical Society). **c** 4D printing that creates thermally responsive shape morphing flower shaped grippers composed of cellulose fibrils alignments programmed hydrogel composite ink (reproduced with permission [93]. Copyright 2016, Springer Nature). **d** 3D printed shape morphing soft grippers that pick-and-place a light ball (reproduced with permission [25]. Copyright 2018, American Chemical Society)

➢ Applications

- Soft actuators (tethered or untethered)

- 포토 리소그래피 및 3D 프린팅 등의 방법은 생체 모방 액추에이터 (biomimetic actuator), 약물 전달 캡슐 (drug delivery capsule), 광전자 센서 (optoelectrical sensor), microsurgical devices, bio-inspired tubular, 인공 장기(artificial organ)와 같은 기능성 소프트 머신을 만드는 연구들이 보고되고 있음.

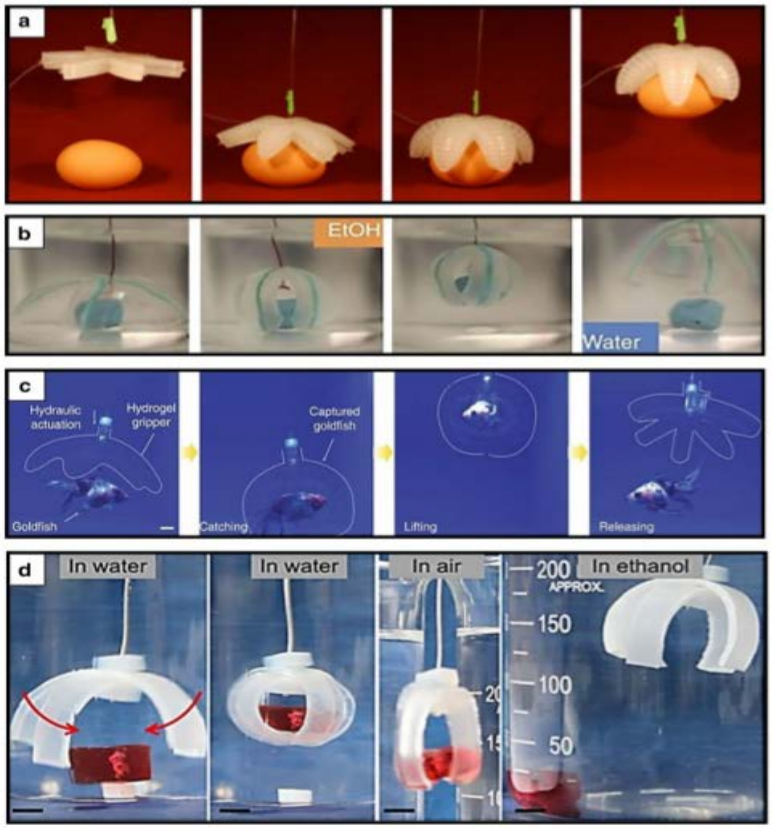

Fig. 5 Tethered soft grippers as smart actuators or manipulators. **a** Pneumatically driven tethered soft gripping robot that provides a range of complex motions by curling upwards or downwards controlled by expansion and contraction in elastomeric structures (reproduced with permission [15]. Copyright 2011, Wiley–VCH). **b** X-shaped ion-printed tethered electrical assistant soft gripper that presents rapid grasp a target in ethanol and releases it in water reversibly (reproduced with permission [99]. Copyright 2013, Springer Nature). **c** Optically and sonically camouflageable hydraulic hydrogel gripping robot that holds and releases a live goldfish noninvasively (reproduced with permission [100]. Adapted with permission under the terms of the Creative Commons Attribution Non Commercial License 4.0 license. Copyright 2017, The Authors). **d** Stimuli responsive ion dip dyeing and transfer printed tough hydrogel-based soft gripper that can fold to grip a target in water and release it in ethanol reversibly (reproduced with permission [101]. Copyright 2016, Wiley–VCH)

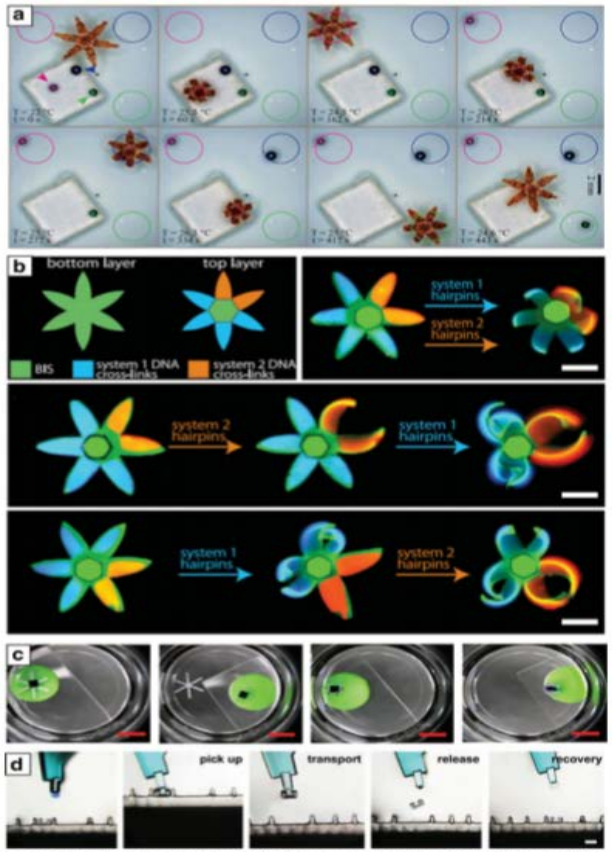

Fig. 6 Untethered soft grippers as smart actuators or manipulators. **a** Thermomagnetically responsive untethered soft gripper that detects and sorts differently colored beads in the respectively colored drop areas autonomously (reproduced with permission [57]. Adapted with permission under the terms of the Creative Commons Attribution Non Commercial License 4.0 license. Copyright 2017, The Authors). **b** Shape programmable DNA-crosslinked untethered soft gripper that presents shape morphing in response to external programmed DNA hairpin sequences (reproduced with permission [102]. Copyright 2017, AAAS). **c** Bifurcation mismatch strain driven shape transformation of stimuli responsive soft gripper that has no hinges in a thin bilayer structure (reproduced with permission [8]. Copyright 2018, Wiley–VCH). **d** Demonstration of the universal pick up, transport, release, and recovery process of a soft robotic microgripper (reproduced with permission [21]. Copyright 2018, Wiley–VCH)

참고 문헌

1. Biomimetic thermal-sensitive Multi-transform Actuator, T. H. Kim, J. G. Choi, J. Y. Byun, Y. Jang, S. M. Kim, G.. M. Spinks & S. J. Kim*, Scientific RepoRts, 9(7905), 2019
2. A Study on the Mold Cooling Circuit Configuration Method Applying Biomimetics, J. H. Choi*, J. S. Gim, B. J. Kim, B. O. Rhee, Conference: KSMTE, 2018
3. Corrigendum: Biomimetic engineering of conductive curli protein films, N.-M. D. Courchesne, E. P. DeBenedictis, J. Tresback, J. J. Kim, A. Duraj-Thatte, D. Zanuy, S. Keten and N. S. Josh, Nanotechnology, 29(45), 2018
4. Surface Engineered Biomimetic Inks Based on UV Cross-Linkable Wood Biopolymers for 3D Printing, W. Xu, X. Zhang, P. Yang, O. Långvik, X. Wang,* Y. Zhang, F. Cheng, M. Österberg, S. Willför, and C. Xu*, ACS Appl. Mater. Interfaces, 11(13), 2019
5. Biomimetic Peptide Nanowires Designed for Conductivity, Rhiannon C. G. Creasey,* A. B.Mostert, A. Solemanifar, T. A. H. Nguyen, B. Virdis, S. Freguia, and B.Laycock*, ACS Omega, 4, 2019
6. Advances in biomimetic stimuli responsive soft grippers, C. Yoon, Nano Convergence, 6(20), 2019